

# Dynamic nucleation and growth of Ni nanoparticles on high-surface area titania

P. Li <sup>a,\*</sup>, J. Liu <sup>b</sup>, N. Nag <sup>c</sup>, P.A. Crozier <sup>d</sup>

<sup>a</sup> TEM Laboratory, Department of Earth and Planetary Sciences, University of New Mexico, MSC03-2040, Northrop Hall, Albuquerque, NM 87131, USA

<sup>b</sup> Monsanto Company, 800 N. Lindbergh Boulevard, St. Louis, MO 63167, USA

<sup>c</sup> Process Technology Group, Engelhard Corporation, 23800 Mercantile Road, Beachwood, OH 44122, USA

<sup>d</sup> Center for Solid State Science, Arizona State University, Tempe, AZ 85287-1704, USA

Received 22 January 2005; accepted for publication 30 November 2005

Available online 27 December 2005

## Abstract

Nucleation and growth mechanisms of Ni nanoparticles synthesized via an incipient wetness technique on a high-surface area titania support (i.e., a mixture of anatase and rutile) are studied using environmental transmission electron microscope (ETEM). Most Ni nanoparticles are found to nucleate from the Ni precursor coated on the surface of the titania support. Even though both anatase and rutile supports are the nucleation sites for Ni nanoparticles, it was observed that the particles have different morphologies on the supports, i.e., a non-wetting morphology on the anatase support versus a wetting morphology on the rutile {101}. This is because the interfacial energy of Ni/rutile is lower than that of Ni/anatase. Titania clusters are found to nucleate on the surface of the Ni particles during in situ ETEM reduction, indicating that the presence of partial titania overlayers is directly related to the synthesis of the Ni/TiO<sub>2</sub> catalysts. The growth mode of the Ni nanoparticles on the titania support is three-dimensional, while that of the rutile cluster on the surface of the Ni is two-dimensional layer-by-layer.

© 2005 Elsevier B.V. All rights reserved.

**Keywords:** Ni; Titanium oxide; Anatase; Rutile; Nucleation; Growth; Morphology; Reduction; Synthesis; Environmental TEM; Nanoparticles; Catalysts

## 1. Introduction

A considerable body of work [1–6] has been carried out on the nucleation and growth of metal clusters on single crystal oxide surfaces due to the extensive applications of metal/oxide systems to heterogeneous catalysts. However, in many practical applications, heterogeneous catalysts are synthesized via an incipient wetness technique on a high-surface area oxide support [7]. This approach uses a combination of wet chemistry and reducing atmospheres to create a dispersion of metal particles and is very different from the ultra-high vacuum (UHV) evaporation techniques used in most of the single crystal work. Very few atomic level studies have been undertaken to understand the

fundamental physical processes taking place during such synthesis. This is partly due to the complex nature of the high-surface area supports, which may consist of particles with different sizes, crystal facets and structures. The problem is compounded by the lack of suitable in situ techniques for studying the transformation process under suitably high gas pressures.

Ni is an important transition metal that is used in many heterogeneous catalysts. In many applications, Ni is loaded on a reducible oxide support like titania. There are a significant number of surface science studies conducted under UHV conditions on the {110} rutile surface [1–6,8,9]. However, in catalytic applications, the metal is usually loaded onto a suitable high-surface area titania. One of the more commonly used titanias is Degussa P25 consisting of 75% anatase and 25% rutile grains [10]. It was suggested that Ni nanoparticles grow three-dimensionally on rutile

\* Corresponding author. Tel.: +1 505 2777536; fax: +1 505 2778843.  
E-mail address: [pengli@unm.edu](mailto:pengli@unm.edu) (P. Li).

supports [2]. However, the growth mechanism of Ni nanoparticles on anatase grains does not appear to have been studied. There are many questions surrounding the nucleation and growth of Ni nanoparticles on the surface of these industrially important high-surface area titanias. Does the precursor uniformly spread over the surface of the support? Is the precursor mobile when heated in a reducing environment? Where are the nucleation sites for metal particle growth? Does the precursor transform directly to metal or are intermediate compounds first formed? These questions and many others remain about not just the Ni on titania but also many other catalytic metal/support combinations.

Environmental transmission electron microscopy (ETEM) is a suitable technique for studying the nucleation and growth of metal nanoparticles on a high-surface area support. The technique allows us to study gas–solid reactions at atomic level with pressures up to a few Torr [10–15] and temperatures up to 800 °C. It is ideal for studying reactions on high-surface area supports because the evolution of individual metal nanoparticles on particular grains of titania can be followed during *in situ* reduction of the precursor. We have already demonstrated that ETEM can be applied to investigate the *in situ* synthesis of Ni nanoparticles from heavy Ni precursor loadings (i.e., 10 wt.%) supported on high-surface area titania [10]. In that study, Ni precursor, loaded by the incipient wetness technique, was found to distribute non-uniformly on the titania support and large patches of Ni precursor acted as nucleation centers for the Ni nanoparticle growth [10]. Most Ni particles were found to possess a non-wetting morphology on the titania support [10]. Modification of the particle equilibrium shape under different gas conditions was also explored [10].

Here we are interested in studying the nucleation and growth process under lower, more realistic metal loadings (3 wt.%). In the present study, we report on the mechanism, at the atomic scale, of the dynamic nucleation and growth of Ni nanoparticles on both anatase and rutile grains. The wetting/non-wetting behavior of the Ni nanoparticles on rutile/anatase supports is discussed in detail. The growth mode of the Ni nanoparticles on rutile and anatase supports is discussed in terms of the surface and interface energies. The growth mode of the Ni nanoparticles on a high-surface area rutile support is compared with UHV single crystal studies. We also observe a double nucleation event in which rutile simultaneously nucleates on the surface of the growing Ni particle. This observation provides evidence for the decoration model proposed [16] to explain the strong metal support interaction (SMSI) associated with metal nanoparticles on reducible oxide supports. The relevance of this decoration model for SMSI phenomena is discussed.

## 2. Experimental procedures

### 2.1. Preparation of precursor

Degussa P-25 (titanium dioxide with a mixture of about 75% anatase and 25% rutile) was loaded with 3 wt.% Ni by

an incipient wetness technique. An aqueous solution containing  $\text{Ni}(\text{NO}_3)_2 \cdot 6\text{H}_2\text{O}$  was added to fill the pores of a certain amount of titania support during constant mixing. After the solution was added, the wet mass was left on an evaporating dish for 30 min in open air. The material was then dried in air at 120 °C for 16 h in a drying oven. Precursor specimens for ETEM were prepared by placing the powders on 50-mesh Pt grids with 99.997% purity.

### 2.2. *In situ* synthesis of Ni metal nanoparticles

To study the dynamic nucleation and growth mechanism of the Ni nanoparticles, the  $\text{Ni}(\text{NO}_3)_2 \cdot 6(\text{H}_2\text{O})$  was reduced *in situ* using a Tecnai F-20 field emission ETEM operating at 200 kV. The microscope has a Scherzer resolution of 0.24 nm with an information limit of 0.12 nm. Precursor samples were loaded into an Inconel heating holder and inserted into the built-in environmental cell between the objective lens pole pieces of the microscope. This arrangement allows us to study the chemical reactions between gas molecules and nanoparticles at reasonably high pressures and reaction temperatures without compromising the atomic resolution imaging capability of the transmission electron microscope (TEM).

*In situ* metal particle synthesis was carried out by reducing the  $\text{Ni}(\text{NO}_3)_2 \cdot 6(\text{H}_2\text{O})$  in 0.2 Torr of CO in the ETEM. The precursor was rapidly heated to 350 °C over a period of 5 min and kept at this temperature in the CO atmosphere for 5 h. For this precursor, CO is a stronger reducing agent than  $\text{H}_2$  and leads to an easier reduction of precursor at lower pressures. Comparison of experiments conducted in  $\text{H}_2$  and CO show no evidence for the precursor reduction being strongly influenced by the formation of  $\text{Ni}(\text{CO})_4$ . In addition, the boiling point of  $\text{Ni}(\text{CO})_4$  is 43 °C and we anticipated that it rapidly decomposes at the reduction temperature employed here (i.e., 350 °C).

The dynamic reduction process of the precursor (i.e., nucleation and growth of Ni nanoparticles) was recorded using a high-resolution camera. Since the formation of individual Ni particles was followed at the atomic level to understand the dynamic reduction process, we were normally able to analyze about 20–30 nucleation and growth events by conducting the experiments under the same reducing condition twice. In order to avoid the strong electron beam introduced artifacts to our experiments, very low electron doses were used to observe the precursor reduction process with some sacrifices of the quality of the high-resolution electron microscopy (HREM) images. HREM images from different areas of the sample were extracted frame by frame from the digital videotape using the IMovie™ software. In some cases, a four-frame averaging process was used to reduce noise. HREM images were also acquired from a CCD camera using DigitalMicrograph 3.1™ software during the ETEM experiments.

The shape of the Ni particles can be clearly determined if the Ni particles locate on the titania surfaces with edge-on orientation, i.e., the titania surface paralleled to the elec-

tron beam direction or viewing direction. This is also the orientation for clearly exploring the interface structures between the Ni particles and the titania support. We were able to place a 1 nm electron probe on particles or clusters extended to the vacuum of the microscope (i.e., particles on the edge of the supports) to perform precise electron energy loss spectroscopy (EELS) chemical analysis of the particles.

### 2.3. TEM imaging of the ex situ Ni/TiO<sub>2</sub> catalysts

We also performed ex situ experiments in which samples were reduced at atmospheric pressure in a mixture of 4% hydrogen and nitrogen at 250 °C, 500 °C and 800 °C. TEM samples were prepared by placing the catalyst powders on holey-carbon films supported on Cu grids. Regular TEM and Z-contrast imaging of the reduced samples were performed in a JEOL 2010F 200 kV Schottky field emission TEM operating in the regular TEM mode and scanning transmission electron microscope (STEM) mode using an electron probe size of 0.2 nm. Z-contrast images are formed by collecting the high-angle electron scattering which has a dependence on the atomic number, *Z*, of approximately  $Z^{1.7}$  [17], hence, the image contrast is sensitive to the presence of heavier nanoparticles (i.e., high-*Z*) on the lighter support. This technique was demonstrated to be able to observe single atoms and small nanoclusters [18] and is used to explore the distribution of Ni nanoparticles on the titania support. The Gatan DigitalMicrograph 3.7.1™ software was used for acquiring the regular TEM and Z-contrast images.

## 3. Results

The HREM images in Fig. 1 give the time evolution of the nucleation and growth of a Ni nanoparticle on a

rutile grain as a result of the reduction of the Ni precursor (i.e., Ni(NO<sub>3</sub>)<sub>2</sub> · 6(H<sub>2</sub>O)). As shown in Fig. 1(a), 30 min into the carbon monoxide reduction, the Ni nanoparticle has nucleated on the rutile {101} surface, where the 0.25 nm and 0.20 nm lattice spacing indicated in the figure corresponds to {101}<sub>rutile</sub> and {111}<sub>Ni</sub> planes, respectively. As time passes (Fig. 1(b)), the area of the Ni/rutile interface increases with concomitant growth of the Ni particle along all the directions. The Ni particle tends to align its {111} atomic planes to the {101} atomic planes of the rutile support, as demonstrated by the parallel {111}<sub>Ni</sub> and {101}<sub>support</sub> across the interface between the Ni nanoparticle and the rutile support in the figure.

Many Ni nanoparticles have also been found to nucleate on the anatase support, as representatively shown in Fig. 2. The lattice spacing of 0.35 nm indicated in Fig. 2(a) corresponds to {101}<sub>anatase</sub> atomic planes. The titania support (i.e., anatase) is coated by a surface overlayer indicated by arrows in the figure. Fig. 2(b) shows that within 20 min of carbon monoxide contact, a Ni nanoparticle with lattice spacing of 0.20 nm corresponding to {111}<sub>Ni</sub> has nucleated at the surface of the titania support from the coated surface overlayer, shown in Fig. 2(a). Notice that the Ni particle nucleates on the rough anatase surface (indicated by a black arrow in Fig. 2(a)) instead of the flat {101}<sub>anatase</sub>. As time passes, the surface overlayer disappears in Fig. 2(c). This strongly suggests that the surface overlayer in Fig. 2(a) and (b) is the Ni precursor that is steadily depleted during reduction with concomitant growth of Ni particles. Also note from Fig. 2(d) that the Ni particle is well-faceted and low energy surface facets, such as the {111} surface facet indicated in the figure, are distinguishable. Two-dimensional layer-by-layer growth

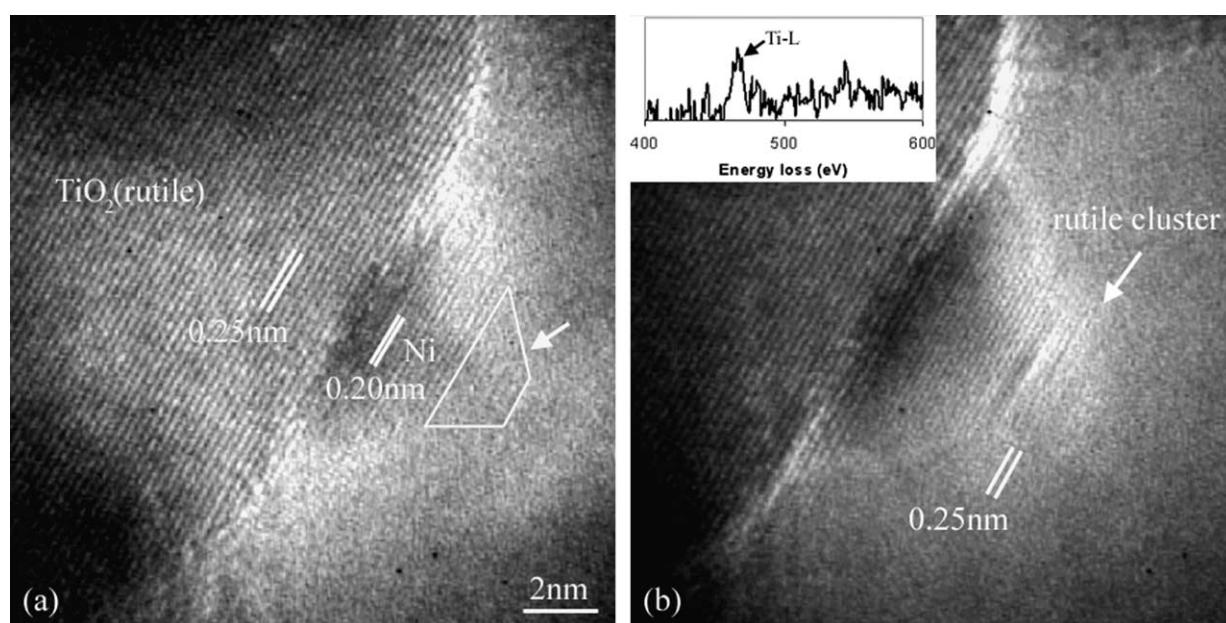


Fig. 1. In situ HREM images showing the nucleation and growth of Ni particles on rutile support after the reduction of the precursor for (a) 30 min and (b) 60 min. Note the superimposed EELS spectrum in Fig. 1(b) acquired from the rutile cluster contains a Ti peak.

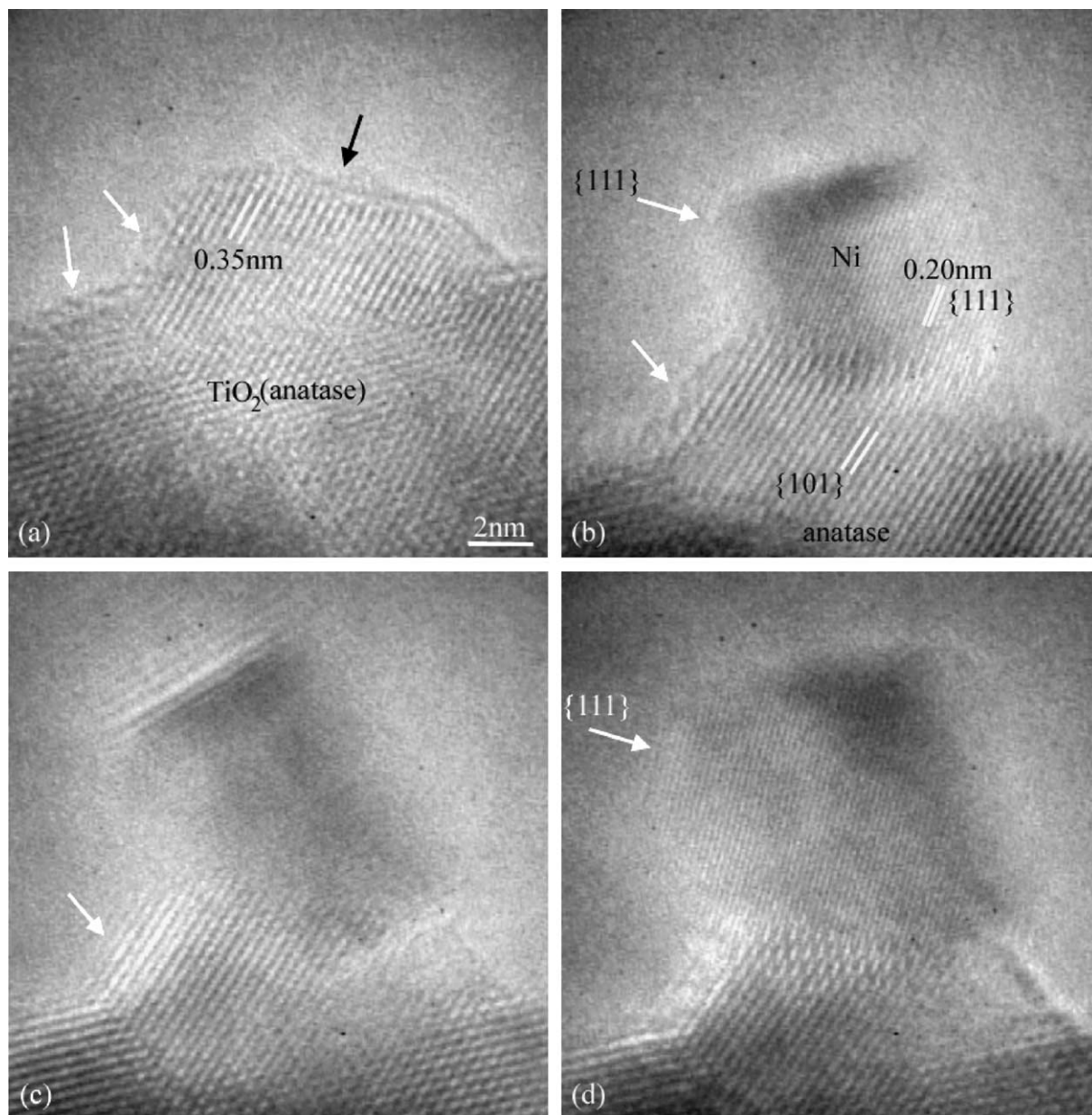


Fig. 2. A series of in situ HREM images showing the nucleation and growth of Ni particles on anatase support: (a) before the reduction, and (b)–(d) after the reduction of the precursor for 20 min, 52 min, and 96 min.

of the Ni nanoparticles has not been observed through the whole synthesis process and the Ni particles grow as three-dimensional nanoislands.

The presence of patches of precursor on some areas of the titania support indicate that the precursor loading was not perfectly uniform. Even though most Ni nanoparticles (i.e., 22 in 24 observations) nucleate from the thin layer of Ni precursor that uniformly coats the titania support, a small number of the Ni nanoparticles (i.e., 2 in 24 observations) transformed directly from the patches of the precursor. In this case, there is a direct relationship between the location of the Ni nanoparticle (indicated by a white arrow in Fig. 3(b)) and the precursor (indicated by a white arrow in Fig. 3(a)), i.e., the Ni nanoparticle stays

at the original location of the Ni precursor. It is also found that the Ni nanoparticle does not move around at this reduction temperature (i.e., 350 °C) and the dynamic particle sintering or coalescence has not been observed.

As demonstrated in Fig. 1, an additional cluster sometimes nucleates at the surface of the Ni nanoparticles supported on both anatase and rutile supports (i.e., in this case, the fuzzy materials indicated by a white arrow in Fig. 1(a)). This phenomenon occurred on the surface of about 20% of the Ni nanoparticles observed (i.e., 5 in 24 observations). The cluster grows with time, as shown in Fig. 1(b). The lattice fringe from this cluster has exactly the same spacing as {101} planes of the rutile support (i.e., 0.25 nm), which is clearly exposed in Fig. 1(b) suggest-

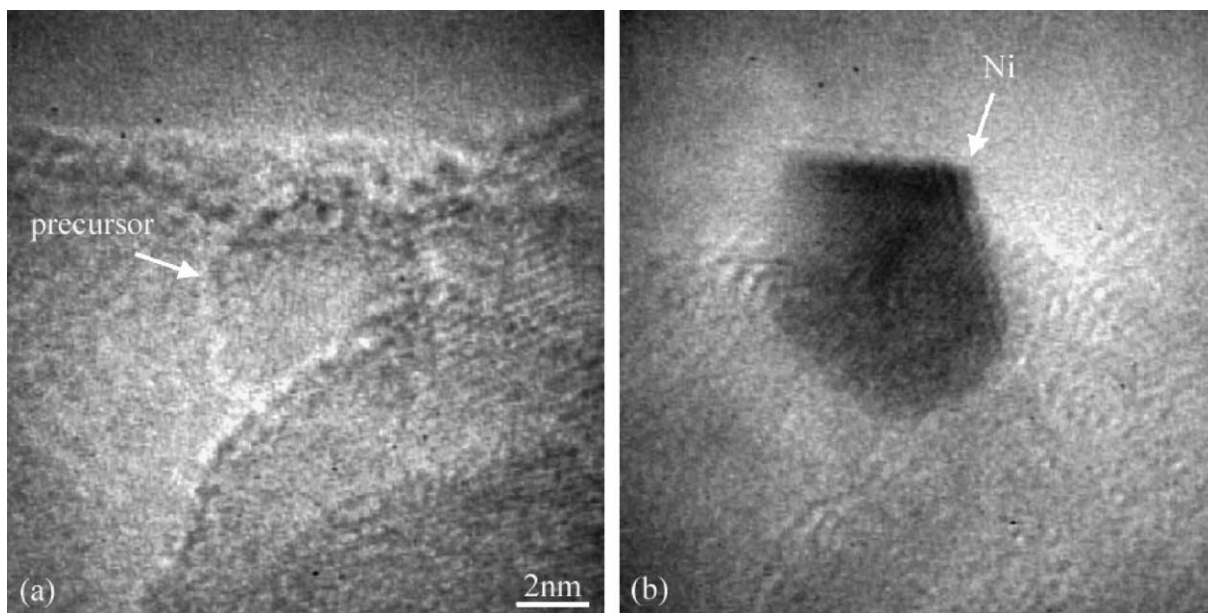


Fig. 3. In situ HREM images showing the direct nucleation of Ni particles from one patch of the precursor on titania support: (a) before the reduction and (b) after the reduction of precursor for 50 min.

ing that this additional cluster is rutile. Furthermore, EELS spectrum acquired from this tiny cluster (see Fig. 1(b)) by precisely placing a 1 nm electron nanoprobe in the center of it, although noisy, shows a Ti peak confirming the rutile interpretation. More importantly, this rutile cluster also tends to align its  $\{101\}$  atomic planes to the  $\{111\}$  atomic planes of the Ni nanoparticles, giving a parallel orientation relationship among the rutile support, Ni nanoparticle and the rutile cluster (i.e.,  $\{101\}_{\text{support}} \parallel \{111\}_{\text{Ni}} \parallel \{101\}_{\text{cluster}}$ ).

The rutile cluster in Fig. 1(a) is already five or six monolayers high and occupies the entire Ni $\{111\}$  surface. In this case the initial growth of the first one or two monolayers of the cluster was not recorded due to the thermal drifting of the specimen holder during the first 20 min of heating. However, the dynamic growth mode of this rutile cluster on the surface of the Ni nanoparticle was observed at a later time and the result is shown in Fig. 4. Notice in Fig. 4(a), an atomic ledge with height about two or three  $\{101\}_{\text{rutile}}$  atomic planes forms at the surface of the titania cluster (indicated by a white arrow), and as time passes (Fig. 4(b)), the surface steps on the titania cluster grows to a complete  $\{101\}_{\text{rutile}}$  terrace. This growth process repeats and the titania cluster continuously grows as seen in Fig. 4(c) and (d).

Another important phenomenon is the different shapes of the Ni nanoparticles on different types of titania supports. In general, the morphology of the supported metallic particles has two types of shape, i.e., non-wetting and wetting. The morphology of the particle is defined to be non-wetting when the contact angle between the metallic particles and support are larger than  $90^\circ$  [16]. As demonstrated in Fig. 2(d), all Ni particles observed in this study (i.e., all eight observations of Ni particles locating on the anatase surfaces with edge-on orientation) possess a non-wetting morphology on anatase surfaces, while the shape

of the Ni particle was wetting in Fig. 1(b) when supported on the rutile  $\{101\}$ , which holds for the two observations of Ni particles locating on rutile  $\{101\}$  with edge-on orientation. Also notice that the  $\{111\}$  Ni atomic planes are not oriented with the  $\{101\}$  anatase planes in Fig. 2(d), while there is a one-dimensional matching of the atomic plane orientation across the Ni/rutile interface in Fig. 1(b). The shape of the Ni particles is directly related to the Ni/titania interface structures, which is discussed in the next section.

The results from our ex situ analysis performed on the hydrogen-reduced samples are in qualitative agreement with our in situ measurements. Regular TEM and Z-contrast imaging of the ex situ samples (in Fig. 5) show average Ni particle sizes of 2 nm, 59 nm and 81 nm corresponding to reduction at 250 °C, 500 °C and 800 °C respectively. The average size on the Ni particles obtained from in situ reduction in CO at 350 °C is 10 nm. Our in situ measurements show that Ni particles nucleate on both anatase and rutile supports (shown in Figs. 1 and 2) during reduction in CO at 350 °C. The ex situ data also shows this trend. Fig. 5(a) and (b) are two representative TEM images of Ni/TiO<sub>2</sub> system after ex situ reduction at 250 °C. In these images, the size and distribution of the 1–2 nm Ni particles are uniform over all titania grains (i.e., 75% anatase grains mixing with 25% rutile grains) demonstrating that the particles nucleate on both anatase and rutile.

## 4. Discussions

### 4.1. Nucleation and growth mechanism of Ni nanoparticles on titania support

Most Ni nanoparticles nucleate from the Ni precursor uniformly coating the titania support, even though a small

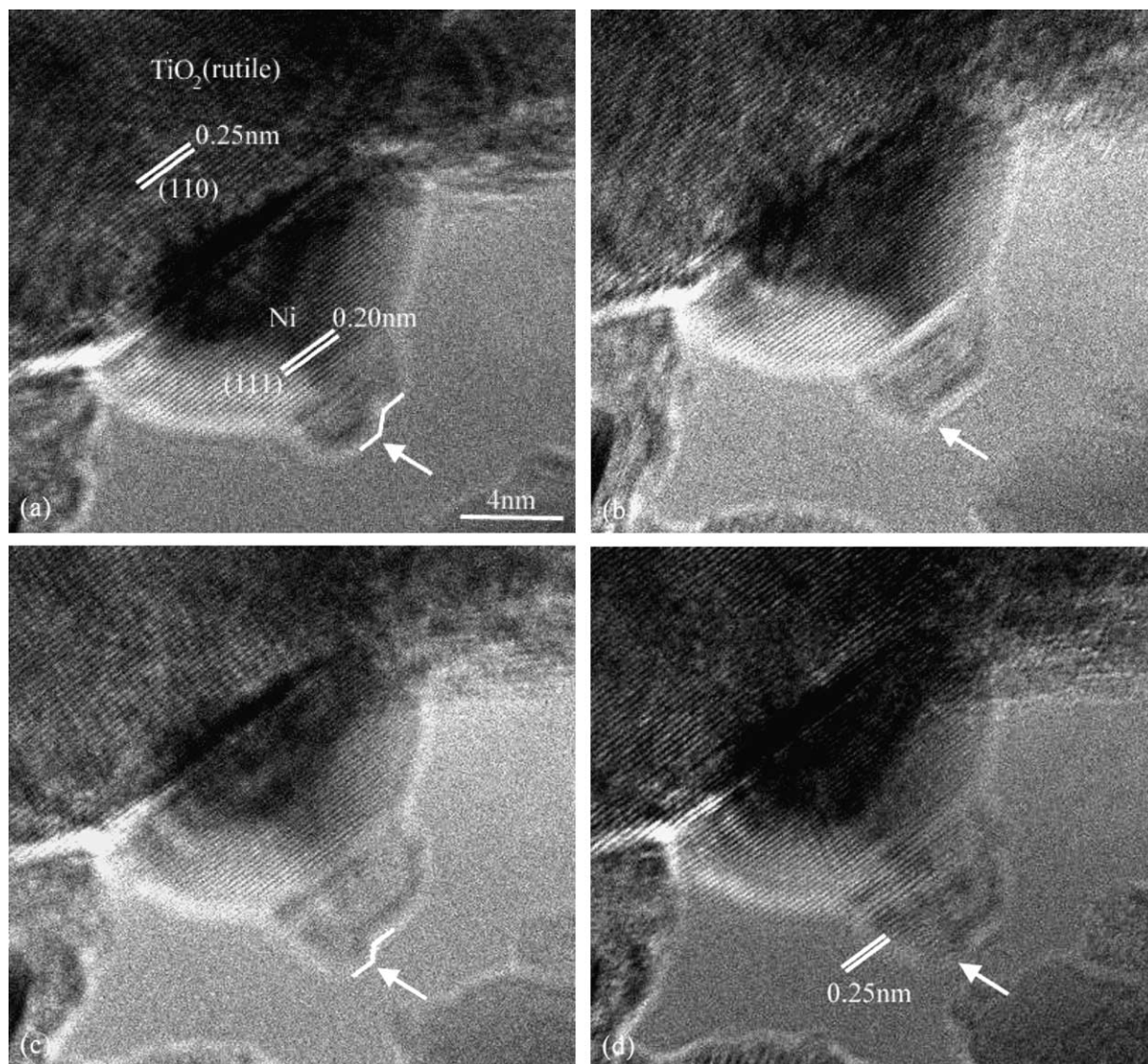


Fig. 4. In situ HREM images showing growth of a titania crystallite on a Ni surface after the precursor was reduced for (a) 180 min, (b) 200 min, (c) 210 min, and (d) 220 min.

number of Ni nanoparticles are directly transformed from the patches of the precursor. This is in contrast to the nucleation process that we observed on samples with higher metal loading where the precursor had a non-uniform distribution on the titania support and the large precursor patches were the nucleation centers for the metal particles [10].

As presented in Section 3, Ni nanoparticles nucleate on both anatase and rutile support in the CO environment. Regular TEM and Z-contrast imaging on the ex situ reduced Ni/TiO<sub>2</sub> catalysts under H<sub>2</sub>/N<sub>2</sub> also demonstrates a uniform distribution of the Ni nanoparticles on the titania supports. Even though the particle size distributions are different, the results indicate that Ni particles do not preferentially nucleate on either anatase or rutile under both CO and H<sub>2</sub> environments. This is different from that in Au/TiO<sub>2</sub> catalyst system, where Au was found to preferentially nucleate only on the rutile support [19]. Ni nanopar-

ticles were also found to nucleate on both anatase and rutile in the high Ni loading sample [10].

Even though Ni particles were occasionally observed to nucleate on the flat anatase {101} surface [10], most Ni nanoparticles nucleate on rough anatase surfaces instead of the low energy flat anatase {101} surface, as shown in Fig. 2(b). This is probably because the surface defects (i.e., the ledges and kinks of the surface) can hold the Ni species for a longer time so that the Ni atoms can meet and grow to nuclei [2,6]. We also observe two instances of Ni nucleating on the {101} surface of rutile (i.e., a relatively higher energy surface than {110}<sub>rutile</sub>). Density functional calculations suggest that, for the equilibrium crystal shapes, 56% of the rutile surface should terminate with the low energy {110} facets and 94% of the anatase surface should terminate with the low energy {101} facets [20,21]. The number of observations of Ni nucleation

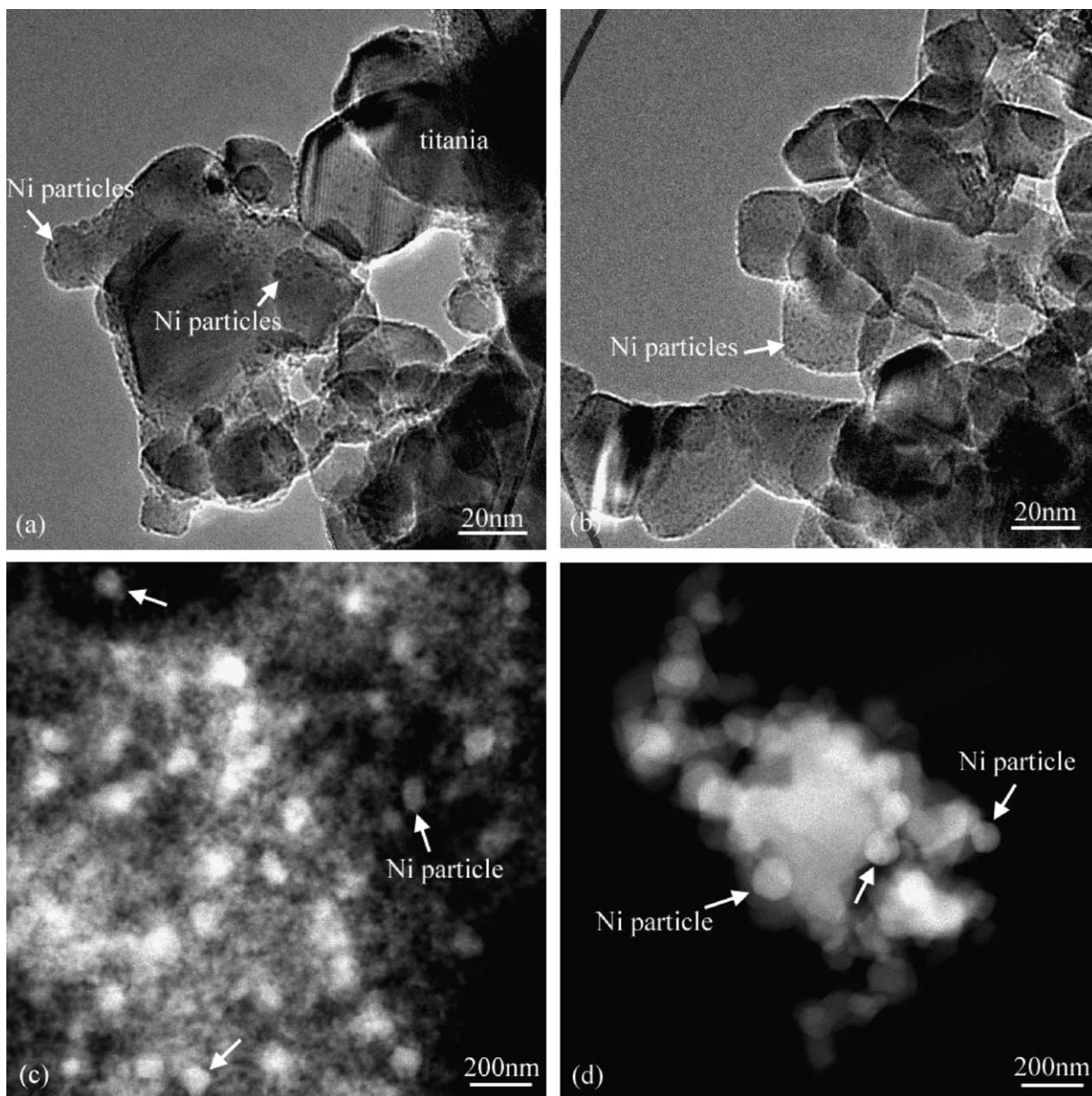


Fig. 5. Regular TEM and Z-contrast images of the 3 wt.% Ni/TiO<sub>2</sub> catalysts ex situ reduced at (a) and (b) 250 °C, (c) 500 °C and (d) 800 °C.

events in which the surface facet can be unambiguously identified is rather small because of the random orientations of the high-surface area support. However, even though the low energy surface of rutile (i.e., {110}) and anatase (i.e., {101}) should compose the majority of the crystal facets, these surfaces do not appear to be the preferential nucleation sites for Ni particles.

The different morphologies of the Ni nanoparticles on anatase and rutile {101} are directly related to the differences in titania surface energies and the Ni/TiO<sub>2</sub> interfacial energies. Typical surface energies for Ni, anatase and rutile along with typical interfacial energies are listed in Table 1. The surface energy of the metal is a function of temperature [22,23]. The experimental value of the Ni surface energy at 0 K was extrapolated from that at high tempera-

ture and the surface energy of Ni solid at the melting point was calculated from that of Ni liquid [22].

The Ni nanoparticles possess a non-wetting or wetting morphology depending on whether  $\gamma_o$  (i.e., the surface energy of the titania) is smaller or larger than  $\gamma_{m/o}$  (i.e., the Ni/TiO<sub>2</sub> interfacial energy) [16]. As is also well known, the interfacial energy is closely related to the interface structure (i.e., atomic matching at the interface) [24], which is qualitatively studied in this work. For all the Ni nanoparticles observed on the anatase support (as shown in Fig. 2(d)), there is no one-dimensional matching of the atomic planes across the Ni/anatase interface. This indicates that the atomic matching may be poor at the interface suggesting that this interface is likely to be incoherent [24,25]. In general, the average surface energy of anatase

Table 1  
Surface energies of Ni, rutile and anatase and interfacial energies

	Free energy (J/m <sup>2</sup> )	Reference and comments
Rutile (average)	1.1	Calculations using local density approximation [20,21]
(110)	0.84	
(100)	1.05	
(101)	1.36	
Anatase (average)	0.9	
(101)	0.84	
(100)	0.96	
Ni (average)	2.24 <sup>1</sup> –2.08 <sup>2</sup>	Data at <sup>1</sup> 0 k and <sup>2</sup> melting point [22]
(111)	2.04	Calculation using EAM potentials [23]
Incoherent interface	0.8–2.5	Generally calculated
Semicoherent interface	0.2–0.8	values [24]
Coherent interface	0.05–0.2	

is about  $\sim 0.9$  J/m<sup>2</sup> [20] and is probably lower than the incoherent interfacial energy (generally ranging from 0.8 to 2.5 J/m<sup>2</sup> [24]) thus generating the non-wetting morphology of the Ni nanoparticles on the anatase support. The non-wetting morphology of Ni particles on flat anatase surface was also demonstrated to be energetically favored by Li et al. [10], where the shape of the Ni particle transforms from wetting to non-wetting on a flat anatase {101} as the reducing time. For the Ni nanoparticles supported on the {101}<sub>rutile</sub>, the surface energy is much larger ( $\sim 1.36$  J/m<sup>2</sup> [20]) compared to the corresponding surfaces for anatase. Moreover, the alignment of the {111}<sub>Ni</sub> and {101}<sub>rutile</sub> planes make it more likely for atoms inside both planes to match at the interface thus lowering the interfacial energy. The comparatively high {101}<sub>rutile</sub> surface energy and low interfacial energy makes it thermodynamically favorable for the Ni nanoparticles to possess a wetting morphology on the {101}<sub>rutile</sub>. It has been found that Cu nanoparticles possess a similar wetting morphology on the ZnO support under a gas mixture of 95% H<sub>2</sub> and 5% CO, where the parallel atomic planes across the Cu/ZnO interface has been observed [12].

The three-dimensional island growth is favored when  $\gamma_o < \gamma_m + \gamma_{m/o}$ , where  $\gamma_o$  and  $\gamma_m$  are the surface energies of titania and Ni nanoparticles, respectively, and  $\gamma_{m/o}$  is again the interfacial energy between the Ni nanoparticle and titania [2,3]. Even the lowest surface energy of Ni (i.e., lowest {111} surface energy of  $\sim 2.04$  J/m<sup>2</sup> [23]) is higher than the surface energies of the most probable titania surfaces (see Table 1). Consequently, the Ni nanoparticles usually grows three-dimensionally on the titania support, even though the Ni/titania interfacial energy is low in some specific cases (i.e., Ni on rutile {101} in this study).

The Ni precursor coated on the titania surface near the initially nucleated Ni nanoparticles is consumed as the metal particle grows. Furthermore, dynamic particle sintering or coalescence is not responsible for the growth of the

Ni nanoparticles since the Ni particles did not move during the observation at 350 °C. This indicates that the growth of the Ni nanoparticles involves the diffusion of the Ni containing species to the surface of the growing metal particles. The mobile Ni species could be either Ni containing precursor molecules or Ni metal atoms produced as a result of the reduction of the precursor. The growth process of Ni nanoparticles can be compared to that in the deposition process of the metallic adatoms on the oxide support [1–4,8,26]. These works show that Ni atoms can diffuse on the titania support at 350 °C, since it has been found that the Ni islands deposited via evaporation at 127–177 °C on rutile {110} were substantially bigger than those deposited at room temperature, indicating the Ni adatoms have sufficient energy to diffuse on the titania support at even lower temperature ranges of 127–177 °C [3]. The discussions from the next section suggest that, in our case, a significant fraction of the mobile Ni species is unreduced or partially reduced precursor.

#### 4.2. Growth mechanism of titania clusters on the surface of Ni nanoparticles and its relationship to SMSI

Titania clusters were found to nucleate on the surface of about 20% Ni nanoparticles (i.e., 5 out of 24 observations) during the reduction process. These titania clusters may originate from titania moieties which dissolve in the Ni solution as a result of the constant mixing that takes place during the precursor impregnation process [16]. After the subsequent drying procedure, this wet solution transforms to a dried precursor coating on the surface of the titania supports. As the reduction takes place, Ni precipitates out of the precursor mixture resulting in an increase in the local concentration of titania species around the Ni particle. More precursor species diffuse into the vicinity of the Ni particle and get reduced as they come into contact with the growing Ni particle. This process leads to a build up in the concentration of titanium moieties on the surface of the growing Ni particles and eventually may result in the nucleation of a titania particle on the Ni surface.

We were not able to observe the onset of the growth of the first one or two monolayers of the rutile cluster on Ni{111} surface. However, Fig. 4 indicates that the growth mechanism of the rutile cluster involves two major steps: (1) the nucleation of the ledge at the surface of the rutile cluster, and (2) the diffusion of the rutile moieties (or atoms) to the ledge to grow to a complete terrace. The growth mechanism of the rutile cluster on Ni{111} surface is similar but slightly different to the traditionally defined two-dimensional layer-on-layer growth mode in the deposition process of metallic particles on large single crystal oxide surfaces [6]. The two-dimensional layer-on-layer growth mode requires that the growth of the next monolayer starts after the first monolayer completes [6,27], while in this study, the growth of the rutile cluster on Ni{111} surface involves the completion of two or three monolayers of rutile {101}. We define the growth mode of the

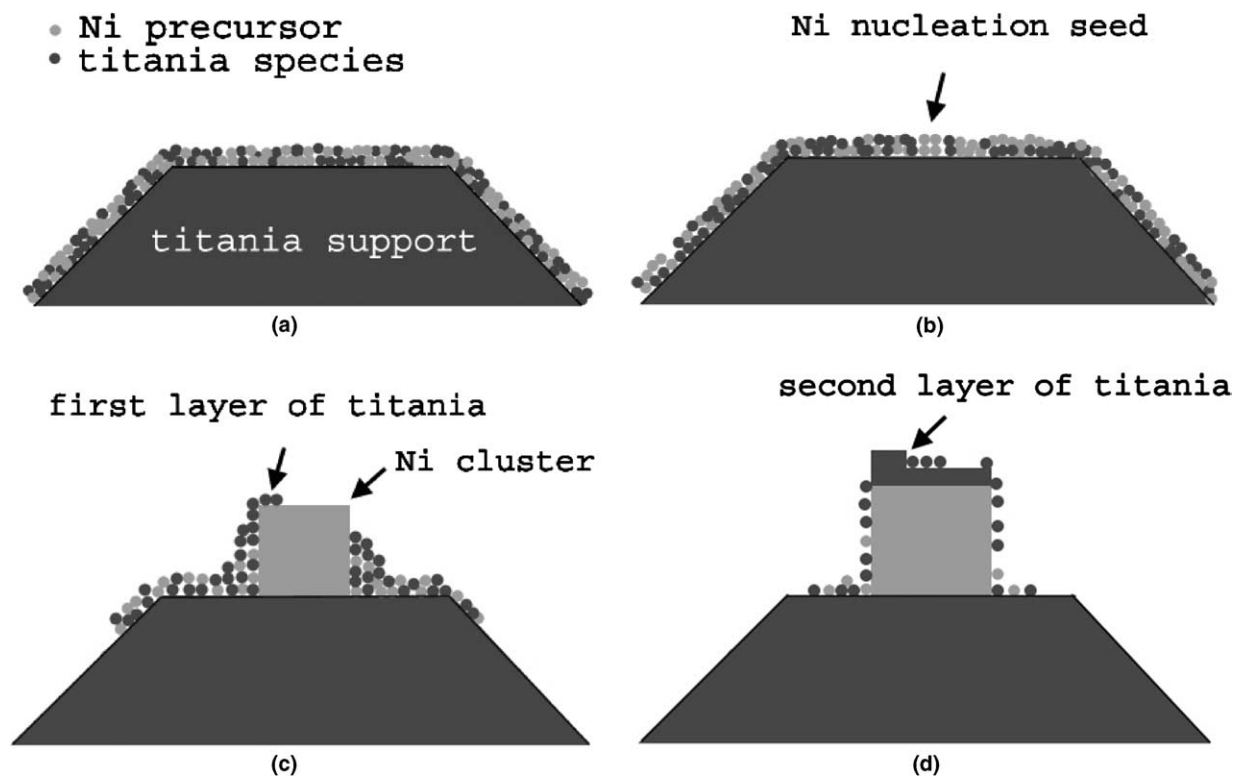


Fig. 6. Illustration of the nucleation and growth of the Ni particle on titania support and the titania cluster on the Ni surface.

rutile cluster on Ni{111} surface to be quasi two-dimensional layer-by-layer. A so-called comparable terrace-ledge growth mechanism has also been frequently observed at heterogeneous solid–solid interfaces and grain boundaries [24]. The dynamic nucleation and growth of the titania cluster on the surface of Ni particles is illustrated in Fig. 6.

The energetics of the growth of rutile clusters on the surfaces of Ni particles is the reverse case of that discussed in Section 4.1 for Ni growing on titania. Two-dimensional layer-by-layer growth of rutile clusters on the surface of the Ni nanoparticles is favored while  $\gamma_{\text{Ni}} > \gamma_{\text{cluster}} + \gamma_{\text{cluster/Ni}}$ , where  $\gamma_{\text{Ni}}$  and  $\gamma_{\text{cluster}}$  are the surface energies of Ni nanoparticle and rutile cluster, respectively, and  $\gamma_{\text{cluster/Ni}}$  is the interfacial energy between the Ni nanoparticle and rutile cluster. In this case, the Ni{111} surface energy is much higher than that of rutile {101} surface (i.e.  $\sim 2.04 \text{ J/m}^2$  [23] versus  $\sim 1.36 \text{ J/m}^2$  [20]) and the Ni/rutile interfacial energy can be low due to the parallel {111}<sub>Ni</sub> and {101}<sub>rutile</sub> at the interface as discussed in Section 4.1. With this configuration of energies, the condition for two-dimensional growth of the rutile cluster on the {111} surface of the Ni nanoparticles can be satisfied. Notice that in this case, the substrate (Ni) has higher surface energy whereas for the Ni on titania case the substrate (titania) has lower surface energy.

It is found that not only the Ni nanoparticle aligns its {111} atomic planes to the {101} atomic planes of the rutile support, but also the rutile cluster on the surface of the Ni nanoparticles tends to align its {101} atomic planes

to the {111} atomic planes of Ni. This indicates that the parallel orientation relationship (i.e., {111}<sub>Ni</sub>||{101}<sub>rutile</sub>) is favorable. Parallel atomic plane matching has not been found for any Ni nanoparticles supported on anatase.

The nucleation of the titania cluster on the Ni surface is probably related to the SMSI phenomenon in Ni/titania system. SMSI was used to describe the drastic changes in the chemisorption properties of group VIII noble metals supported on reducible oxide supports [28]. One common explanation for the SMSI phenomenon is that reduced titania from the support migrates onto the surface of the metal particles [29–32]. Regarding this interpretation, HREM on ex situ reduced catalyst samples have clearly shown the occurrence of titania surface coatings on metal nanoparticle surfaces [33–36]. Our ex situ experiments at 500 °C and 800 °C also show a titania coating on Ni surfaces. In our in situ experiment, significant titania reduction is unlikely to occur at the temperature of 350 °C used in this study (titania reduction normally occurs at temperatures above 500 °C [16]). However, it has already been suggested that small amounts of titania species may dissolve in the impregnation solution and be deposited onto the surface of the metal particle during reduction [16]. Our results support this hypothesis and show that nucleation of at least some titania clusters on the surface of the Ni particles takes place during catalyst synthesis. However, our results also show that only a small number of Ni particles have titania particles on their surfaces suggesting that this mechanism may make only a small contribution to the SMSI phenomena.

## 5. Conclusions

Nucleation and growth mechanisms for synthesis of Ni nanoparticles on a high-surface area titania support (i.e., a mixture of anatase and rutile) have been studied at atomic resolution. It was found that most Ni nanoparticles nucleate from a thin uniform Ni precursor coating on the surface of the titania support. A minority of Ni particles nucleated directly from irregular patches of the Ni precursor which were also present on the titania support. Ni particles nucleated on both anatase and rutile grains although low energy oxide surfaces do not appear to be preferential nucleation sites. Ni nanoparticles showed a non-wetting morphology when nucleated on the anatase support, while it was observed that Ni nanoparticles possess a wetting morphology when nucleated on the rutile {101}. This is due to the one-dimensional atomic plane matching across the Ni/rutile interface causing a lowering of the interfacial energy. The Ni nanoparticles grow as three-dimensional islands and growth involves the surface diffusion of the Ni species. Titania clusters have also been found to nucleate on the surface of the growing Ni particles, indicating that titania overlayers on metal particles can be directly related to the synthesis of the Ni/TiO<sub>2</sub> catalysts. The growth of the rutile cluster on the surface of the Ni particle follows the two-dimensional layer-by-layer growth mode.

## Acknowledgements

This research was conducted using the facilities in the Center for Solid State Science at Arizona State University and was supported by Monsanto Company. The authors thank Mr. K. Weiss for the maintenance of the Tecnai F-20 ETEM. The authors also thank Dr. R. Sharma and Dr. R.-J. Liu for the valuable discussions regarding the ETEM.

## References

- [1] A. Kolmakov, D.W. Goodman, *The Chemical Record* 2 (2002) 446.
- [2] R.E. Tanner, I. Goldfarb, M.R. Castell, G.A.D. Briggs, *Surf. Sci.* 486 (2001) 167.
- [3] J. Zhou, Y.C. Kang, D.A. Chen, *Surf. Sci.* 537 (2003) L429.
- [4] C. Xu, X. Lai, G.W. Zajac, D.W. Goodman, *Phys. Rev. B* 56 (1997) 13464.
- [5] C.R. Henry, *Surf. Sci. Rep.* 31 (1998) 235.
- [6] C.T. Campbell, *Surf. Sci. Rep.* 27 (1997) 1.
- [7] A.J. Van Dillen, R.J. Terörde, D.J. Lensveld, J.W. Geus, K.P. Jong, *J. Catal.* 216 (2003) 257.
- [8] M. Wu, P.J. Møller, *Surf. Sci.* 279 (1992) 23.
- [9] U. Diebold, J. Pan, T.E. Madey, *Surf. Sci.* 331–333 (1995) 845.
- [10] P. Li, J. Liu, N. Nag, P.A. Crozier, *J. Phys. Chem. B* 109 (2005) 13883.
- [11] P.L. Gai, *Adv. Mater.* 10 (1998) 1259.
- [12] P.L. Hansen, J.B. Wagner, S. Helveg, J.R. Rostrup-Nielsen, B.S. Clausen, H. Topsøe, *Science* 295 (2002) 2053.
- [13] P.L. Gai, *Top. Catal.* 8 (1999) 97.
- [14] E.D. Boyes, P.L. Gai, *Ultramicroscopy* 67 (1997) 219.
- [15] R. Sharma, *Microsc. Microanal.* 7 (2001) 494.
- [16] G.B. Raupp, S.A. Stevenson, J.A. Dumesic, S.J. Tauster, R.T.K. Baker, Metal-support interactions, in: S.A. Stevenson, J.A. Dumesic, R.T.K. Baker, E. Ruckenstein (Eds.), *Catalysis, Sintering, and Redispersion*, Van Nostrand Reinhold Company Inc., New York, NY, 1987.
- [17] E.J. Kirkland, *Advanced Computing in Electron Microscopy*, Plenum Press, New York, NY, 1998.
- [18] P.D. Nellist, S.J. Pennycook, *Science* 274 (1996) 413.
- [19] T. Akita, P. Lu, S. Ichikawa, K. Tanaka, M. Haruta, *Surf. Interface Anal.* 31 (2001) 73.
- [20] M. Lazzeri, A. Vittadini, A. Selloni, *Phys. Rev. B* 63 (2001) 155409.
- [21] M. Ramamoorthy, D. Vanderbilt, R.D. King-Smith, *Phys. Rev. B* 49 (1994) 16721.
- [22] W.R. Tyson, W.A. Miller, *Surf. Sci.* 62 (1977) 267.
- [23] M.I. Baskes, *Phys. Rev. B* 46 (1992) 2727.
- [24] J.M. Howe, *Interfaces in Materials: Atomic Structure, Kinetics and Thermodynamics of Solid:Solid, Solid:Liquid and Solid:Vapor Interfaces*, John Wiley and Sons, New York, NY, 1997.
- [25] P. Li, J.M. Howe, W.T. Reynolds Jr., *Acta Mater.* 52 (2004) 239.
- [26] Q. Zhu, A. Zhang, E.D. Williams, R.L. Park, *Surf. Sci.* 172 (1986) 433.
- [27] F.C. Frank, J.H. van der Merwe, *Proc. Roy. Soc. (London)* A198 (1984) 205.
- [28] S.J. Tauster, S.C. Fung, R.L. Garten, *J. Am. Chem. Soc.* 100 (1978) 170.
- [29] R.T.K. Baker, J.J. Chludzinski, J.A. Dumesic, *J. Catal.* 93 (1985) 312.
- [30] J.A. Dumesic, S.A. Stevenson, R.D. Sherwood, R.T.K. Baker, *J. Catal.* 99 (1985) 79.
- [31] S. Bernal, J.J. Calvino, M.A. Cauqui, J.M. Gatica, C. Lpez, J.A. Pérez Omil, J.M. Pintado, *Catal. Today* 77 (2003) 385.
- [32] D. Olga, H. Wilhelm, D. Ulrike, *Phys. Rev. Lett.* 84 (2000) 3646.
- [33] A.D. Logan, E.J. Braunschweig, A.K. Datye, D.J. Smith, *Langmuir* 4 (1988) 827.
- [34] E.J. Braunschweig, A.D. Logan, A.K. Datye, D.J. Smith, *J. Catal.* 118 (1989) 227.
- [35] S. Bernal, F.J. Botana, J.J. Calvino, C. López Cartes, J.A. Pérez Omil, J.M. Rodríguez-Izquierdo, *J. Chem. Soc., Faraday Trans.* 92 (1996) 2799.
- [36] S. Bernal, J.J. Calvino, M.A. Cauqui, J.M. Gatica, C. López Cartes, J.A. Pérez Omil, J.M. Pintado, *Catal. Today* 77 (2003) 385.